Coupled plastic flow and phase transformation under compression of materials in a diamond anvil cell: Effects of transformation kinetics and yield strength

Oleg M. Zarechnyy, Valery I. Levitas, and Yanzhang Ma

Citation: J. Appl. Phys. **111**, 023518 (2012); doi: 10.1063/1.3677977
View online: http://dx.doi.org/10.1063/1.3677977
View Table of Contents: http://jap.aip.org/resource/1/JAPIAU/v111/i2
Published by the American Institute of Physics.

Coupled plastic flow and phase transformation under compression of materials in a diamond anvil cell: Effects of transformation kinetics and yield strength

Oleg M. Zarechnyy,[1] Valery I. Levitas,[2,a)] and Yanzhang Ma[3]
[1]*Iowa State University, Department of Aerospace Engineering, Ames, Iowa 50011, USA*
[2]*Iowa State University, Department of Aerospace Engineering, Mechanical Engineering, and Material Science and Engineering, Ames, Iowa 50011, USA*
[3]*Department of Mechanical Engineering, Texas Tech University, Lubbock, Texas 79409, USA*

(Received 15 September 2011; accepted 15 December 2011; published online 31 January 2012)

The large-strain problem on phase transformations (PTs) under compression in a diamond anvil cell is studied in detail using the finite-element method. The combined effect of transformation kinetics and ratios of the yield strengths of low- and high-pressure phases is examined. Some experimental phenomena (e.g., plateaus in pressure distribution and plastic flow to the center of a sample) are reproduced. Results are applied to interpretation of experimental data and characterization of strain-induced PTs. © *2012 American Institute of Physics*. [doi:10.1063/1.3677977]

I. INTRODUCTION

Most phase transformation (PT) studies under high pressure are performed in diamond anvil cell (DAC) (Fig. 1(a)) during sample compression. As an increase in pressure p is caused by a large irreversible reduction in sample thickness, a large plastic flow precedes and accompanies PTs. It was recently recognized[1] that such PTs should be considered as strain-induced (rather than pressure-induced), i.e., they occur via nucleation at new defects continuously generated during plastic flow. This causes completely different thermodynamic and kinetic description as well as experimental characterization in comparison with pressure-induced PTs. The concept of phase-equilibrium pressure is not relevant for strain-induced PTs. The latter are characterized in terms of the strain-controlled, pressure-dependent kinetic equation in Eq. (10), which depends on three main parameters: the minimum pressure p^d_ε, below which direct strain- induced PT is impossible, the maximum pressure p^r_ε, above which reverse strain-induced PT is impossible, and parameter k, which determines the magnitude of transformation rate. Due to very heterogeneous distributions of all fields in a sample,[2–4] it is very difficult to experimentally determine such an equation or even the main parameters of it. That is why theory and finite-element method (FEM) simulations have been developed to study evolution of all fields and interpret experimental data.[2–4] Despite the significant success, results in Refs. 2–4 fail to describe a number of experimentally observed phenomena. Thus, in experiments,[5,6] a plateau (step) in pressure distribution in the two-phase region is observed in KCl and fullerene, and the corresponding pressure p_p is called PT pressure. Simulations in Refs. 2–4 reproduced these plateaus for compression and shear in rotational DAC, but did not observe them for compression for $\sigma_{y2}/\sigma_{y1} \geq 1$, where σ_{y1} and σ_{y2} are the yield strengths of the low- and high-pressure phases. However, the physical sense of the pressure at the step p_p is not clear. Next, it was concluded in Refs. 2–4 that it is impossible to determine key parameters, p^d_ε and p^r_ε, from a compression experiment, and, finally, plastic flow to the center of a sample, which is often observed in experiments, was not reproduced. Since simulations can be performed for just some generic material parameters, the key question is whether the above contradictions are due to missing physics or the improper choice of parameters. Also, while the effect of change in σ_{y2}/σ_{y1} was studied in Refs. 2–4 for $k = 1$ and was nontrivial, the effect of kinetic parameter k was not studied and may change some conclusions in Refs. 2–4. The goal of this letter is to study the combined effect of kinetics and σ_{y2}/σ_{y1} on the coupled plastic flow and PTs and resolve the above-mentioned problems. Both experimental phenomena mentioned above, plastic flow to the center of a sample and plateaus in pressure distribution for all σ_{y2}/σ_{y1}, were obtained in simulations. In some cases, pressure at steps corresponds to p^d_ε, but in other cases does not, and it is difficult to distinguish the former from the latter. For $\sigma_{y2}/\sigma_{y1} = 0.2$, at the lowest step, $p = p^r_\varepsilon$ in the two-phase region, but reverse PT was not observed. It was found that accelerated kinetics drastically affect the evolution of morphology of transforming regions, plastic flow, and stress distribution, as well as interpretation of experimental data.

The model, problem formulation, and FEM approach for coupled plastic flow and PT in a sample of radius R compressed between two rigid diamonds are presented in detail in Refs. 2 and 3. The total system of equations includes the following equations:
Kinematic decomposition:

$$\boldsymbol{d} = \overset{\nabla}{\boldsymbol{\varepsilon}}_e + \dot{\varepsilon}_t \boldsymbol{I} + \boldsymbol{d}_p; \tag{1}$$

Hooke's elasticity rule:

$$p = K\varepsilon_{e0}; \quad \boldsymbol{s} = 2G\, dev\boldsymbol{\varepsilon}_e; \tag{2}$$

Von Mises yield condition:

a)Author to whom correspondence should be addressed. Electronic mail: vlevitas@iastate.edu.

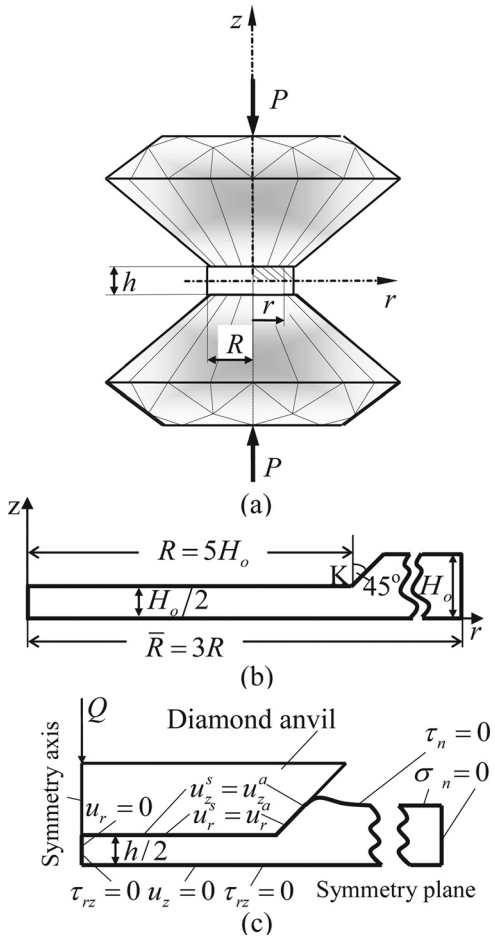

FIG. 1. Diamond anvil cell (DAC) model (a), sample in initial undeformed state (b), and boundary conditions (c).

$$\sigma_i := \left(\frac{3}{2}\boldsymbol{s}:\boldsymbol{s}\right)^{0.5} \le \sigma_y(c), \tag{3}$$

$$\sigma_y := (1-c)\sigma_{y1} + c\sigma_{y2}; \tag{4}$$

Associated plastic flow rule in the elastic regime:

$$\sigma_i < \sigma_y(c); \quad \boldsymbol{d}_p = 0; \tag{5}$$

in the plastic regime:

$$\sigma_i = \sigma_y(c); \quad \boldsymbol{d}_p = \lambda \boldsymbol{s}; \tag{6}$$

Consistency condition:

$$\dot{\sigma}_i = \dot{\sigma}_y \Rightarrow \lambda = \frac{3}{2}\frac{\boldsymbol{s}:\boldsymbol{d}}{\sigma_y^2} - \frac{(\sigma_{y2}-\sigma_{y1})\dot{c}}{\sigma_y G}; \tag{7}$$

Transformation strain:

$$\varepsilon_t = \bar{\varepsilon}_t c; \tag{8}$$

Equilibrium equation:

$$\nabla \cdot \boldsymbol{T} = 0. \tag{9}$$

Strain-controlled kinetic equation is accepted in the form

$$\frac{dc}{dq} = 10k\frac{(1-c)\bar{p}_d H(\bar{p}_d)\dfrac{\sigma_{y2}}{\sigma_{y1}} - c\bar{p}_r H(\bar{p}_r)}{c + (1-c)\sigma_{y2}/\sigma_{y1}}, \tag{10}$$

$$\text{where} \quad \bar{p}_d = \frac{p - p_\varepsilon^d}{p_h^d - p_\varepsilon^d} \quad \text{and} \quad \bar{p}_r = \frac{p - p_\varepsilon^r}{p_h^r - p_\varepsilon^r}.$$

Equation (1) represents decomposition of deformation rate $\boldsymbol{d}$ into elastic, transformational, and plastic $\boldsymbol{d}_p$ contributions, where $\boldsymbol{I}$ is the unit tensor and $\overset{\nabla}{\boldsymbol{\varepsilon}}_e$ is the Jaumann objective time derivative of the elastic strain; K and G are the bulk and shear moduli, the same for both phases; $\boldsymbol{s}$ is the deviatoric part of the Cauchy stress tensor $\boldsymbol{T}$; ε_{e0} is the volumetric elastic strain and $dev\boldsymbol{\varepsilon}_e$ is the deviatoric part of the elastic strain tensor; σ_i is the stress intensity; σ_y is the yield strength of the mixture of low- and high-pressure phases; $\bar{\varepsilon}_t$ is the volumetric transformation strain; H is the Heaviside step function; p_h^d and p_h^r are the pressures for direct and reverse PTs under hydrostatic conditions, c is the volume fraction of the high-pressure phase with respect to undeformed volume; and q is the accumulated plastic strain.

Below, all parameters with dimensions of stress were normalized by σ_{y1}; we used $p_\varepsilon^d = 6.75$, $p_\varepsilon^r = 6.375$, $p_h^d = 11.25$, $p_h^r = 1.875$, and $k = 5$, 10, and 30. In all cases, plastic flow to the center of the sample occurs at some stage of compression that corresponds to the experiments, in contrast to $k = 1$ in Refs. 2 and 3. This plastic flow is caused by a faster volume decrease due to PT rather than due to compression; it also changes pressure and concentration distributions.

II. PT TO THE WEAKER PHASE

For all k, a small portion of high-pressure phase $c < 0.001$ appears first at the center of the sample, as with $k = 1$ (Refs. 2 and 3). Subsequently, in contrast to Refs. 2 and 3, the main PT progress then shifts from the sample center (Fig. 2) and occurs at the plane of symmetry. For $k = 5$, PT propagates from the plane of symmetry toward the

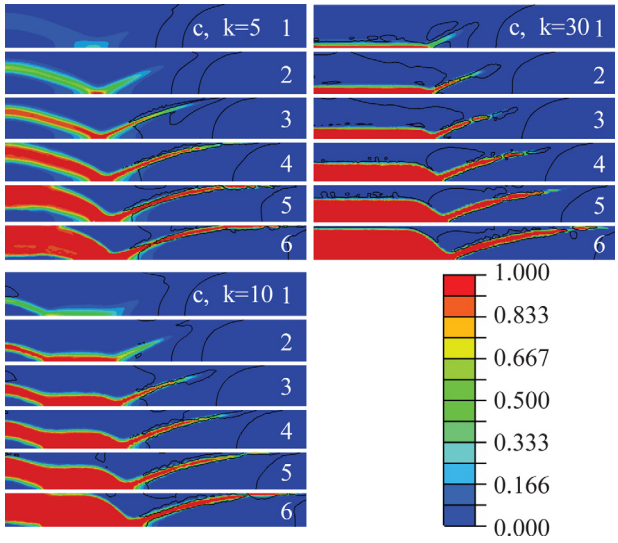

FIG. 2. (Color online) Concentration of high-pressure phase for $k = 5$, 10, and 30 and $\sigma_{y2} = 0.2\sigma_{y1}$, $r/R \le 0.64$. The dimensionless axial force F normalized by cullet area and σ_{y1} is 4.09 (1), 4.23 (2), 4.37 (3), 4.54 (4), 4.71 (5), and 4.97 (6). Between the black lines, $p_\varepsilon^r < p < p_\varepsilon^d$ and PT does not occur.

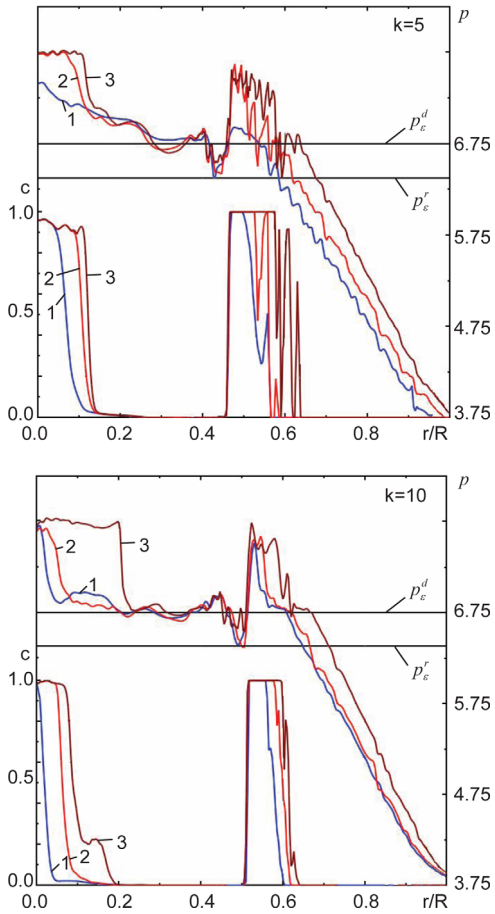

FIG. 3. (Color online) Distributions of pressure p and high-pressure phase concentration c for $\sigma_{y2}=0.2\sigma_{y1}$; $k=5$, $F=4.54$ (1), $F=4.72$ (2), $F=5.02$ (3); $k=10$, $F=4.84$ (1), $F=4.88$ (2), and $F=5.16$ (3).

contact surface along two shear bands. Such a localization of PT is caused by strain localization, due to the reduction in strength during PT. PT regions reach the contact surface at the later stage of PT (in contrast to $k=1$), which prevents its detection with the help of surface-based (e.g., optical and Raman) methods. Thus, x ray methods can only be used for detection of PT in the early stage. The strain and PT localization zone that is directed toward the sample periphery does not reach the contact surface; at some stage, an isolated transformed region appears at the contact surface and coalescence of two regions occurs through the plastic flow of the transformed material rather than being due to PT. Pressure distribution (Fig. 3) possesses numerous fluctuations, similar to the case of $k=1$, that are caused by multiple plastic instabilities due to material softening.

Several steps appear at pressure distribution at the contact surface; some of them correspond to p_ε^d, but some do not. When the PT region reaches the contact surface, plateaus in pressure distribution appear in these regions. The pressure values at the three plateaus barely change during loading and become approximately the same for all k, which gives an erroneous impression that these values characterize PTs. Moreover, two of these steps appear in the region of transformed material when it reaches the contact surface. However, pressure is equal to p_ε^d at one plateau only in the area at the surface where PT did not occur.

Pressure on other plateaus is determined by the mechanics of PT interaction and plastic flow rather than corresponding to fundamental PT parameters in the kinetic equation in Eq. (10). At the fourth (the lowest) step, $p=p_\varepsilon^r$ in the two-phase region, while reverse PT was not observed. Still, this can be used to determine p_ε^r from the experiment. Results in Fig. 3 exhibit the main features of the wavy experimental plot for *ZnSe* (Ref. 7) (see also supplementary Fig. 9 in Ref. 4): monotonous pressure growth from periphery to center, a drop followed by a step, and subsequent growth until the next plateau at the sample center. A very small, transformed region can be observed visually at the contact surface near the center,[7] similar to Figs. 2 and 3; however, quite a large region inside of the sample may also transform (Fig. 2). It is hard to say which step (if any) in Ref. 7 corresponds to p_ε^d.

Remarkably, for $k=30$, the moving transformation front that fully separates transformed and untransformed regions is horizontal. Pressure grows in the entire transforming region, despite the volume decrease. This, however, does not contradict the Le Chatelier principle of equilibrium thermodynamics, as it is not applicable to strain-induced PTs.[2,4] While, in Refs. 2 and 4 we obtained pressure growth despite the volume decrease for $\sigma_{y2}=5\sigma_{y1}$ and anvil rotation, which could be explained with the help of a simplified model,[1,8,9] the current result does not allow for such an interpretation, as a simplified model is not applicable for $\sigma_{y2}=0.2\sigma_{y1}$.

III. PT FOR THE CASES WITH $\sigma_{y2}/\sigma_{y1}\geq 1$

Unlike in Refs. 2 and 3 for $k=1$, steps in pressure distribution (Fig. 4) are observed for $\sigma_{y2}=\sigma_{y1}$ and $\sigma_{y2}=5\sigma_{y1}$ and for $k=5$, 10, and 30. The steps start developing for $k=5$, become well defined for $k=10$, and even better for $k=30$. In all cases, they are located within the two-phase region between the fully transformed and untransformed phases, with pressure slightly above p_ε^d, which can be used for an approximate evaluation of p_ε^d from the experiment. However, there are other steps in other regions with higher p, so it is difficult to make a choice in the experimental curve which step corresponds to p_ε^d. Distributions of contact shear (friction) stresses τ_{zr} for $\sigma_{y2}=\sigma_{y1}$ and $k=5$, 10, and 30 are presented in Fig. 5 for the several axial forces F.

At the periphery, $\tau=\tau_{y1}$ and shear is localized near and along the contact surface, imitating a sliding along the diamond surface from the center.[2–4] An increase in k causes a slight increase in c in practically the same region, which leads to the reduction in shear stresses and changes their sign in some regions, because of intense volume reduction due to PT. This is consistent with the flow to the center in the volume of the sample (Fig. 6).

At further compression, the plastic flow changes direction several times and finally is directed toward the periphery. Such a sequence takes place at different stages of compression for all σ_{y2}/σ_{y1} and $k=5$, 10, and 30. For $k=10$ and 30, the later stage of compression, and in the two-phase region, contact shear stress drops due to volume reduction, producing a local stagnation zone. Such a plastic flow toward the center and, later, toward the periphery of the sample completely changes the PT evolution in the sample. For $k=1$ in Ref. 2, plastic

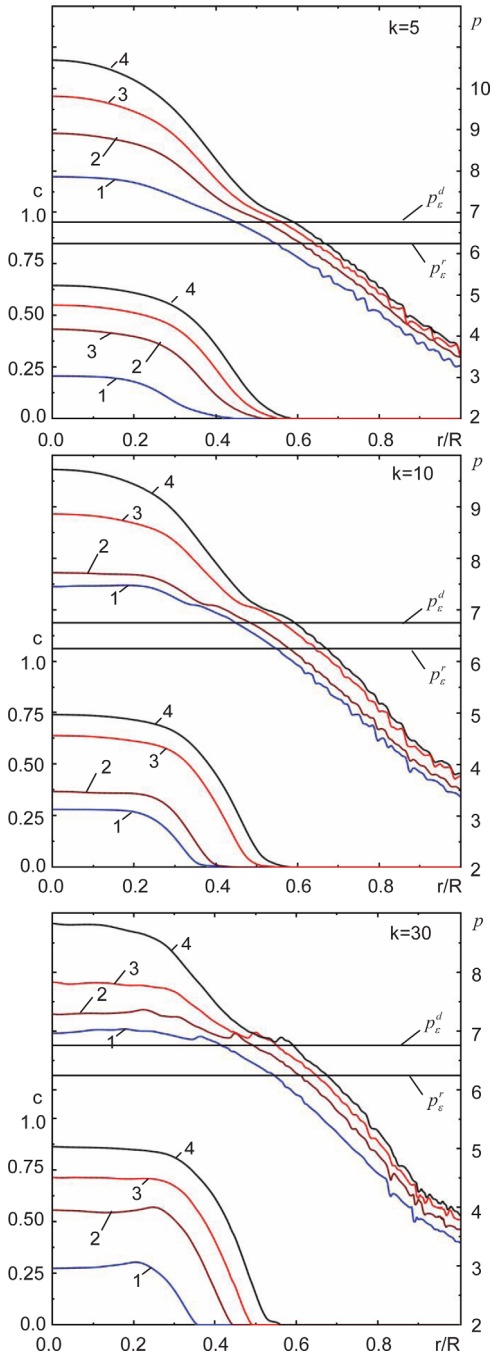

FIG. 4. (Color online) Distributions of pressure p and high-pressure phase c for $\sigma_{y2}=5\sigma_{y1}$ and $k=5$, 10, and 30. The axial force F is 4.44 (1), 4.91 (2), 5.22 (3), and 5.52 (4).

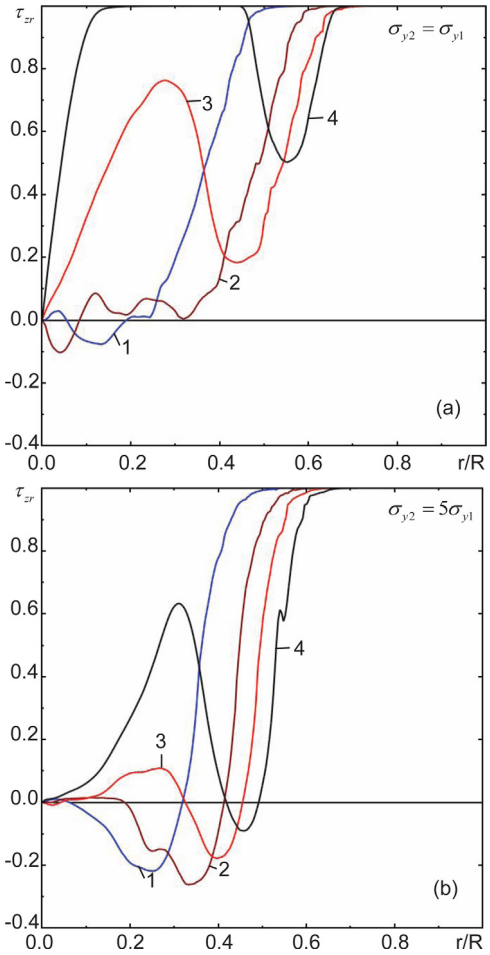

FIG. 5. (Color online) Distribution of shear stress τ_{zr} for $k=30$, $\sigma_{y2}=\sigma_{y1}$ (a), and $\sigma_{y2}=5\sigma_{y1}$ (b). The axial force F is 4.44 (1), 4.91 (2), 5.22 (3), and 5.52 (4). For convenience, shear stresses are normalized by the yield strength in shear $\tau_{y1}=\sigma_{y1}/\sqrt{3}$.

flow was always directed away from the center; therefore, the transformed region at the contact surface was much larger than at the plane of symmetry.[2,3] Here, the transforming region initially propagates faster along the plane of the symmetry rather than along the contact surface; when flow changes to the one from the center, propagation of the transforming region at the contact surface is catching up with its propagation at the symmetry plane, and later it progresses similar to $k=1$ in Refs. 2 and 3. The increase in k leads to a more uniform phase distribution along the height at later stages of compression. To conclude, accelerated kinetics drastically affect the evolution of the morphology of transforming regions, plastic flow, and stress distribution, as well as the possibility of interpretation of experimental data. Thus, for all cases, plastic flow to the center of the sample occurs at some stage of compression, which corresponds to the experiments. While the evolution of geometry in the transforming zone for $\sigma_{y2}/\sigma_{y1}\geq 1$ at a later compression stage is qualitatively the same for any $1\leq k\leq 30$, it changes qualitatively for PT to a weaker phase. Thus, surprisingly, PT completes at the symmetry plane away from the center and, subsequently, a completely transformed region grows and reaches contact surface with an anvil at the very late compression stage. Thus, this prevents the possibility of early-stage PT detection by surface-based methods (optical and Raman) and leaves x ray detection as the only possible choice. Several steps are observed at quite a noisy pressure distribution at the contact surface, some of which correspond to p^d_ε, but some of which do not. Pressure values at three plateaus remain almost constant during loading and virtually the same for all k, which gives an erroneous impression that these values characterize PTs. However, pressure is equal to p^d_ε at just one plateau only (in the region at the surface, where PT did not start) and pressure on other plateaus do not correspond to any characteristic pressure in the kinetic equation in Eq. (10). Moreover, one of these plateaus appears in the region of transformed material when it reaches the contact surface. Regardless, pressure at

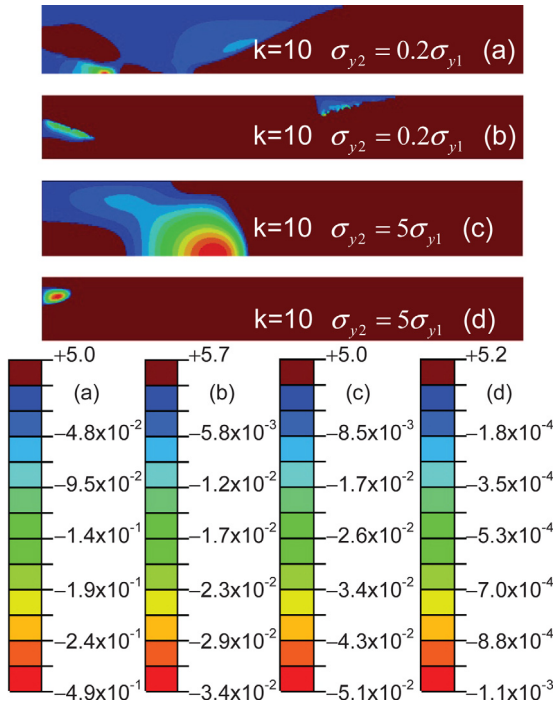

FIG. 6. (Color online) Distribution of radial velocity v_r for $k=10$ in the central part of the sample for $r/R \leq 0.64$; (a) $\sigma_{y2}=0.2\sigma_{y1}$, axial force $F=4.09$; (b) $\sigma_{y2}=0.2\sigma_{y1}$, axial force $F=4.71$; (c) $\sigma_{y2}=5\sigma_{y1}$, axial force $F=4.09$; (d) $\sigma_{y2}=5\sigma_{y1}$, and axial force $F=4.71$. The brown zone designates the region where plastic flow occurs from the center ($v_r>0$).

this plateau is approximately $1.1p_\varepsilon^d$ and determined by mechanics of PT interaction and plastic flow rather than corresponding to fundamental PT parameters in the kinetic equation in Eq. (10). Surprisingly, at the fourth, lowest step, $p=p_\varepsilon^r$ in the two-phase region, while reverse PT was not observed. Nevertheless, this observation can be used to determine p_ε^r from the compression experiment. For $k=30$, pressure grows in the entire transforming region, despite the volume decrease. This does not contradict the Le Chatelier principle, as it is not applicable to strain-induced PTs.[2,4] For $\sigma_{y2}/\sigma_{y1} \geq 1$, a step in pressure distribution was reproduced and became more pronounced as k increased, which is why it was not observed in Refs. 2 and 3 for $k=1$. This step is also located in the two-phase region and is slightly above p_ε^d, which can be used for approximate evaluation of p_ε^d from the experiment. However, there are other steps with higher pressure in different regions and it is difficult to determine which step corresponds to p_ε^d in an experimental curve. Thus, the obtained results demonstrate the strong effect of kinetics, reproduce some experimental features that were not reproduced in Refs. 2 and 3, offer new insight, and demonstrate some existing problems in the interpretation of experimental data.

ACKNOWLEDGMENTS

The support of Army Research Office (Grant No. W911NF-09-1-0001 managed by Dr. David Stepp and Dr. Suveen Mathaudhu), Defense Threat Reduction Agency (Grant No. HDTRA1-09-1-0034 managed by Dr. Su Peiris), and Iowa State University is gratefully acknowledged.

[1]V. I. Levitas, Phys. Rev. B **70**, 184118 (2004).
[2]V. I. Levitas and O. M. Zarechnyy, Europhys. Lett. **88**, 16004 (2009).
[3]V. I. Levitas and O. M. Zarechnyy, Phys. Rev. B **82**, 174123 (2010).
[4]V. I. Levitas and O. M. Zarechnyy, Phys. Rev. B **82**, 174124 (2010).
[5]V. D. Blank, Y. Y. Boguslavski, M. I. Eremetz, E. S. Izkevich, Y. S. Konyaev, A. M. Shirokov, and E. I. Estrin, Sov. Phys. JETP **87**, 922 (1984).
[6]N. V. Novikov, S. B. Polotnyak, L. K. Shvedov, and V. I. Levitas, J. Superhard Mater. **3**, 39 (1999).
[7]V. D. Blank and S. G. Buga, Instrum. Exp. Tech. **36**, 149 (1993).
[8]V. I. Levitas, J. Mech. Phys. Solids **45**, 1203 (1997).
[9]V. I. Levitas, J. Mech. Phys. Solids **45**, 923 (1997).